Accepted Manuscript

Synthesis and ionic conductivity of new high Li ion content garnets, $LnSr_2Ta_2Li_7O_{12}$ (Ln = La, Pr, Nd, Sm, Gd)

M.A. Howard, O. Clemens, A.S. Parvathy, P.A. Anderson, P.R. Slater

PII: S0925-8388(16)30279-1

DOI: 10.1016/j.jallcom.2016.02.012

Reference: JALCOM 36623

To appear in: *Journal of Alloys and Compounds*

Received Date: 17 September 2015

Revised Date: 30 January 2016

Accepted Date: 2 February 2016

Please cite this article as: M.A. Howard, O. Clemens, A.S. Parvathy, P.A. Anderson, P.R. Slater, Synthesis and ionic conductivity of new high Li ion content garnets, $LnSr_2Ta_2Li_7O_{12}$ (Ln = La, Pr, Nd, Sm, Gd), *Journal of Alloys and Compounds* (2016), doi: 10.1016/j.jallcom.2016.02.012.

Synthesis and ionic conductivity of new high Li ion content garnets, $LnSr_2Ta_2Li_7O_{12}$ (Ln = La, Pr, Nd, Sm, Gd)

M. A. Howard[a], O. Clemens[a,b,c], A. S. Parvathy[b,c], P. A. Anderson[a], P. R. Slater[a]

[a] School of Chemistry, University of Birmingham, Birmingham, B15 2TT

[b] Technische Universität Darmstadt, Joint Research Laboratory Nanomaterials, Jovanka-Bontschits-Straße 2, 64287 Darmstadt, Germany

[c] Karlsruher Institut für Technologie, Institut für Nanotechnologie, Hermann-von-Helmholtz-Platz 1, 76344 Eggenstein-Leopoldshafen, Germany.

[*]Correspondence to: Prof. P. R. Slater

School of Chemistry, University of Birmingham, Birmingham B15 2TT. UK

Tel. +44 (0)121 4148906

Fax +44 (0)121 4144403

p.r.slater@bham.ac.uk

Abstract

In this paper we report the synthesis and Li ion conductivity of the new high Li content garnet phases $LnSr_2Ta_2Li_7O_{12}$ (Ln = La, Pr, Nd, Sm or Gd). Close inspection of the X-ray diffraction patterns indicate that these systems are mostly composed of the ordered tetragonal garnet phase, along with a small amount of cubic garnet. The presence of a small amount of cubic garnet phase can most likely be correlated with partial Li loss on synthesis as well as some degree of H^+/Li^+ exchange. The latter was supported by results from variable temperature X-ray diffraction studies and thermogravimetric analysis. The adoption of the tetragonal garnet structure by these new systems highlights further that in order to accommodate 7 Lithium ions within the garnet structure, then cation ordering must occur to prevent short Li-Li interactions. In line with other tetragonal garnet systems, the Li ion conductivity is shown to be low, as a result of this ordered Li distribution.

Keywords: Inorganic Materials; Oxide Materials; Ionic Conduction; X-ray diffraction.

1. Introduction

With the increase in demand for high capacity, light weight Li ion batteries for portable electronics such as mobile phones, laptop and tablet devices, there has been an intensive drive to develop new materials in this area. While traditional Li ion batteries adopt liquid electrolytes, there is increasing interest in the development of solid electrolytes, which give rise to opportunities for miniaturisation, along with increased safety. Potential candidates for this application are Li containing materials with the garnet-type structure. While traditional garnets have the general formula $A_3B_2C_3O_{12}$ (A - 8 coordinate, B - 6 coordinate, C - 4 coordinate), these Li ion conducting garnet materials are of particular interest due to their ability to accommodate excess Li^+ cations within the structure. These excess cations are located in new interstitial distorted octahedral positions, with accompanying vacancies in the tetrahedral positions to prevent too short Li-Li interactions. The increased lithium ion content leads to the general formula $A_3B_2Li_{3+x}O_{12}$ $0 \leq x \leq 4$ [1-11]. The first observation of fast Li ion conductivity ($\sigma_{total(25°C)} = 3.4 \times 10^{-6}$ S cm^{-1}) in these systems was reported for $La_3M_2Li_5O_{12}$ (M = Nb, Ta) by Thangadurai and Weppner [12]. The same authors later reported the possibility of increasing the Li content by partial substitution of La (A site) with K or alkaline earth cations, or by substitution of In on the Nb (B site) [13]. As Li has a low scattering factor of X-rays, there was initially much confusion over the distribution across the different Li sites [1, 14]. However, neutron diffraction studies by Cussen *et al.* clarified the structural situation, showing that the Li was located on 3 sites: the ideal garnet tetrahedral and two interstitial distorted octahedral sites [2]. Cussen also showed that the occupancy of the interstitial octahedral sites was vital for high conductivity, since $Ln_3Te_2Li_3O_{12}$ (Ln = rare earth), where the Li is only located on the ideal tetrahedral site, shows poor ionic conductivity [15].

Since early work showed an increase in Li ion conductivity on increasing the Li content, there has been a large amount of research on doping studies to increase the Li content as high as possible (see for example the review article [16]). This research has shown that the maximum Li content achievable is 7 Li per formula unit. Furthermore, it has been reported that at this maximum lithium content, Li cation ordering occurs, resulting in a lowering of symmetry from cubic to tetragonal [7, 9, 17-19]. In

this cell, there is an ordered distribution in which 1 in 3 Li_{tet} sites is occupied, with the remaining 6 Li in the distorted octahedral sites, so as to avoid short Li – Li bond distances. As a result of the Li ordering , the ionic conductivity of such systems is poor [7, 9]. One "Li_7" system that has, however, attracted some controversy is $La_3Zr_2Li_7O_{12}$, with some initial reports of cubic symmetry, with the cubic phase showing high ionic conductivity ($\sigma_{total(25°C)} = 3 \times 10^{-4}$ S cm^{-1}) [20] , much larger than that of the tetragonal phase [9]. The observation of cubic "$La_3Zr_2Li_7O_{12}$" was often reported when high synthesis temperatures were used (up to 1000°C) along with long heating time (more than 12hrs). These high temperatures and long heating times can lead to Li evaporation, and reaction with the Al_2O_3 crucible resulting in a lowering of the Li content from 7, thereby resulting in cubic symmetry. Subsequent reports confirmed Al incorporation from the crucible, and this work was then extended to show that Al, Ga, Ge, In and Si could all be doped onto the Li site [17, 21-30]. A range of other doping strategies have been extended to $La_3Zr_2Li_7O_{12}$, showing high conductivities when the Li content was lowered below 7 and so a cubic system was obtained, although there have still been some claims of the successful synthesis of undoped cubic $La_3Zr_2Li_7O_{12}$, which has caused some confusion as to when cation ordering occurs in these garnets [18,31,32-37].

The conduction mechanism within these Li ion garnets has also attracted significant interest [38-40], and recent NMR studies have demonstrated that all the Li sites (tetrahedral and distorted octahedral) are involved in the conduction process. The strong promise of these garnet electolytes has recently been further demonstrated in their successful operation in Li ion batteries, including the demonstration of their use as composite electrolytes with polymer systems for the production of high voltage bipolar cells [41, 42]

Another interesting feature of these garnet Li ion conductors is their ability to undergo partial H^+/Li^+ exchange [43-46] through either submersion in water or organic acids. The sensitivity towards H^+/Li^+ exchange has been further highlighted by recent reports of this exchange occurring through reaction with moisture in air [44, 45, 47-50]. In this respect, we have previously reported that H^+/Li^+ exchange occurs in Al, Ga doped $(La/Nd)_3Zr_2Li_7O_{12}$ on exposure to air and that this exchange results in changes to the ionic conductivity/issues with sintering [17,18, 28]. We have shown through neutron powder

diffraction studies, that the exchanged protons in $La_3Nb_2Li_5O_{12}$, are found within the distorted octahedral sites of the Li sub-lattice [44].

In this paper, we have investigated the possible synthesis of a range of new "Li_7" garnets, $LnSr_2Ta_2Li_7O_{12}$ (Ln = La, Pr, Nd, Sm, or Gd), in order to confirm the universal adoption of the ordered tetragonal garnet structure for such high Li content systems, and so, once and for all, confirm the need for cation ordering to accommodate 7 Li ions in these garnet systems. We also investigate the conductivities of these systems and their tendency to undergo H^+/Li^+ exchange in air.

2. Experimental

$LnSr_2Ta_2Li_7O_{12}$ (Ln = La, Pr, Nd, Sm or Gd) were synthesised *via* standard solid state synthesis routes. Stoichiometric amounts of La_2O_3, Pr_6O_{11}, Nd_2O_3, Sm_2O_3, or Gd_2O_3, $SrCO_3$, Ta_2O_5, Li_2CO_3 (20% molar excess to account for Li volatility) were ground together with an agate pestle and mortar until a homogeneous mixture was achieved. The ground powder was then transferred into an alumina crucible. The powder was then heated to 600 °C for 2 hours, before raising the heating temperature to 800 °C for 14 hours. The heated powder was then reground with a further 15% molar excess of Li_2CO_3 added. The powder was then pressed into a pellet and placed on top of a ZrO_2 pellet (to prevent reaction with the alumina crucible) and fired again at 850 °C for 12 hours.

Powder X-ray diffraction (PXRD) patterns of the synthesised garnets were collected on a Bruker D8 diffractometer set in transmission geometry with a $CuK_{\alpha 1}$ radiation source in the angular range between 15 and 60 ° 2θ. Unit cell parameters were calculated from the diffraction pattern using the Topas refinement suite [51] by Rietveld analysis (the structural model of tetragonal $La_3Zr_2Li_7O_{12}$ [9] with space group $I4_1/acd$ was employed with Ln and Sr occupying the La site, and Ta occupying the Zr site). In this analysis, only unit cell parameters, shape parameters and an overall scaling factor were refined.

Variable temperature X-ray powder diffraction (VT-XRD) patterns were recorded for $LnSr_2Ta_2Li_7O_{12}$ (Ln = Nd, Pr) on a Bruker D8 diffractometer with Bragg-Brentano geometry and a fine focus Cu X-ray tube, using an Anton Paar HTK 1200N High-Temperature Oven-Chamber in the temperature

range between 30 and 900 °C (intervals of 50 °C). A scan time of 17 minutes per scan was used for the angular range between 10 and 60 ° 2θ. No primary beam monochromator was attached. A VANTEC detector and a fixed divergence slit (0.3 °) were used for the measurements. Prior to measurement, both samples were stored in air in non-gas tight plastic containers for ~1 week. As will be shown, this results in the uptake of water and the formation of additional impurity phases (e. g. $SrCO_3$) due to the resultant changes in composition. Analysis of the VT-XRD data was performed using the Rietveld method with the program TOPAS 4.2 (Bruker AXS, Karlsruhe, Germany) [52]. The instrumental intensity distribution for the X-ray data was determined empirically from a sort of fundamental parameters set [53], using a reference scan of LaB_6, and the microstructural parameters were refined to adjust the peak shapes for the XRD data. The analysis showed that most of the recorded patterns could not be refined properly using only one garnet type phase. Therefore, two phases had to be used to obtain a good fit for the reflections, a tetragonal one and a pseudocubic one. The pseudocubic phase was refined using the same structural model (atomic positions and thermal parameters) as used for the tetragonal phase, while applying a constraint to obtain a pseudocubic cell setting (*i.e.* $a = c$). An independent shape parameter (strain type contribution) was used for the pseudocubic phase. It is worth mentioning that from the quality of the recorded data it is not possible to determine if the pseudocubic phase is indeed truly cubic, or rather tetragonal with a c/a ratio very close to 1.

To complement the VT-PXRD studies, thermogravimetric analysis (coupled with analysis of evolved gases using a mass spectrometer) was carried out using a Netzsch STA 449 F1 Jupiter Thermal Analyser. The $LnSr_2Ta_2Li_7O_{12}$ (Ln = Nd, Pr) samples were heated to 800°C in N_2 with a heating rate of 10°C min^{-1}.

For the A.C. impedance spectroscopy measurements, the garnet phases were pressed as pellets and sintered at 1000°C (on top of a ZrO_2 pellet to prevent reaction with the alumina crucible) for 2 hours. The sintered pellets were coated in a silver paste to ensure good electrical contact between the electrode and the pellet. Silver electrodes were then affixed onto the surface of the painted pellet. A.C. Impedance measurements were carried out using Hewlett Packard 4192A Impedance Analyser over

the frequency ranges 0.1 – 10^3 kHz applied amplitude. The collected impedance data were analysed using Z-plot software [54].

The SEM images were taken using the secondary electron detector of a Philips XL30 FEG scanning electron microscope operating at 20 keV. For SEM experiments, $NdSr_2Ta_2Li_7O_{12}$ was exemplarily chosen to characterize sample morphology of the pellet used for impedance spectroscopy measurements. The sample was sputtered with approximately 10 nm of Au prior to the measurements.

3. Results and discussion

For all $LnSr_2Ta_2Li_7O_{12}$ (Ln = La, Pr, Nd, Sm, Gd) phases, the X-ray diffraction patterns showed peak splitting indicative of the tetragonal garnet unit cell (the XRD pattern for Ln=Nd is shown in Fig. 1a). The results therefore are consistent with the conclusion that "Li_7" systems in general adopt a tetragonal unit cell, which can be explained by the ordered Li distribution in the tetragonal garnet cell helping to ensure that too short Li-Li interactions do not occur [7, 9, 18, 19]. Cell parameters were determined for each system and are given in Table 1. The data show the expected decrease in cell volume on reducing the size of the lanthanide. It should, however, be noted that a close inspection of the X-ray diffraction patterns suggested the presence of some cubic garnet phase (Fig. 1b and 1c), the quantity of which varied from sample to sample. Small amounts of perovskite type impurity phases (1-2 wt-%) were also observed for a number of compounds. This highlights the difficulty in synthesising these high Li content phases, even with high Li excess used, and can be most likely attributed to volatility of Li, which may be enhanced through reaction with moisture in the air.

As detailed in the introduction, there have been a number of reports of H^+/Li^+ exchange occurring in either air atmosphere [17, 18, 28, 47-49] or when these garnets are submerged in an organic acid or water [43-45]. Therefore in order to determine the possibility that the presence of some cubic phase was due to partial H^+/Li^+ exchange, variable temperature PXRD diffraction data were collected from room temperature to 900 °C to observe any changes. Recorded patterns on heating and cooling are presented in Fig. 2 for $NdSr_2Ta_2Li_7O_{12}$. Using these data, Rietveld refinement was employed to estimate the variation in the weight fractions of tetragonal and cubic phases with temperature. Fig. 3a

shows the changes in the calculated weight fraction of the cubic phase with temperature for $NdSr_2Ta_2Li_7O_{12}$ on heating and cooling. For this sample it can be clearly seen that the first heating procedure behaves differently compared to subsequent cooling and heating procedures, with the fraction of cubic phase being significantly higher, especially between 150-400°C. This observation can be correlated with partial H^+/Li^+ exchange with the exchanged Li most likely present on the surface as $LiOH/Li_2CO_3$. The higher weight fraction cubic phases can be correlated then with the fact that this exchange lowers the temperature of the tetragonal-cubic phase transition, as shown previously for $La_3Zr_2Li_7O_{12}$ [48]. On heating above 400°C the protons are lost as water is eliminated and any surface Li most likely reinserts into the structure leading to a decrease in the cubic garnet weight fraction. On further heating above 800°C, there is the expected reversible cubic-tetragonal transition (order-disorder) for the anhydrous $NdSr_2Ta_2Li_7O_{12}$ phase, and the whole sample is now cubic, as also seen previously for $La_3M_2Li_7O_{12}$ (M=Sn, Zr) [7, 48].

The loss of water from the initial heating means that the first cooling experiments and the second heating and cooling experiments show different results, with the %wt. of cubic staying much lower indicating limited H^+/Li^+ exchange has been able to occur. The fact that there remains a small fraction of cubic phase, and the presence of a small amount of $SrCO_3$ impurity, is most likely related to some Li loss on heating and hence some fraction of lower Li content $Nd_{1+x}Sr_{2-x}Ta_2Li_{7-x}O_{12}$ phase. The partial Li^+/H^+ exchange is also highlighted in the cell parameters of the tetragonal phase, suggesting that at low H^+/Li^+ exchange, the tetragonality (c/a ratio) is reduced, with further exchange leading to a cell that is metrically cubic. Fig. 3b shows the c/a for the tetragonal phase component *vs*. temperature. From these data, there are distinct differences between the 1st heating experiment and 1st cooling experiment/2nd heating and cooling experiments. In particular there is a large deviation in the c/a ratio especially in the 150-400°C range on the first heating experiment, consistent with the effect of the presence of a degree of H^+/Li^+ exchange.

A second variable temperature X-ray diffraction experiment was performed on the $PrSr_2Ta_2Li_7O_{12}$ system. For this phase, the evidence for H^+/Li^+ was not quite as visibly apparent as in the Nd sample. However, on close inspection, there was an indication of differences between the XRD data on

heating/cooling, consistent with H^+/Li^+ exchange. In particular, for the first heat treatment, the %wt. fraction of cubic phase (Fig. 4a) in the sample was higher than for the cooling/2nd heating experiment, and there was a slight divergence in the tetragonality (c/a ratio) for the tetragonal phase *vs*. temperature (Fig. 4b).

To complement the VT-PXRD studies, thermogravimetric analysis, coupled with evolved gas analysis through mass spectrometry, was performed on both samples. In both cases a mass loss was observed at ~450°C on heating, which mass spectrometry indicated was due to both H_2O and CO_2 loss. This mass loss corresponds to the significant changes observed from the VT-PXRD studies, which were attributed to water loss and Li reinsertion. The fact that both H_2O and CO_2 are lost can be attributed to the initial H^+/Li^+ exchange leading to surface LiOH which then reacts with CO_2 to give Li_2CO_3. On heating the protons in the garnet are lost and Li reinserts according to the following equation:

$$LnSr_2Ta_2Li_{7-x}H_xO_{12} + x/2Li_2CO_3 \rightarrow LnSr_2Ta_2Li_7O_{12} + x/2\ CO_2 + x/2\ H_2O$$

On the second heating cycle, no mass loss was observed, consistent with the VT-XRD data, which suggested that there was insufficient time to facilitate the H^+/Li^+ re-exchange during the cooling cycle.

Following on from the XRD studies, A.C. impedance spectroscopy measurements were performed in order to determine the conductivities of these $LnSr_2Ta_2Li_7O_{12}$ systems. These measurements were performed on pellets sintered at 1000°C for 2 hours. This sintering regime led to pellet densities of 70-80% theoretical, which are lower than ideal, however attempts to increase the density via higher temperature sintering led to significant Li loss and correspondingly high levels of impurities. SEM measurements, exemplarily performed on $NdSr_2Ta_2Li_7O_{12,}$ show sintered particles with relatively large particle sizes of the order of ~ 5 – 20 µm (see Fig. 5), albeit with significant pellet porosity as noted above. Conductivity measurements were made above 150 °C as below this temperature the resistances were too large to be measured. The Arrhenius plots for all the samples are presented in Fig. 6, with the data showing much lower conductivities compared to previously reported cubic Li containing garnets. The highest conductivity was observed for the $PrSr_2Ta_2Li_7O_{12}$ sample ($\sigma_{bulk(150\ °C)}$ = 1.5×10^{-5} S cm^{-1}). The calculated activation energies ranged from 0.74 – 0.94 eV, much higher than

values reported for cubic garnets (Ea = 0.3 – 0.4 eV [1-3, 8, 12, 13, 55]). While, as noted above, the pellet densities were comparatively low, which might be expected to contribute to a lowering of the conductivity, the conductivity values obtained are substantially lower than those observed for comparatively sintered cubic garnets [16,17]. Thus a major contribution to the low ionic conductivity and high activation energies can be attributed to the ordering on the Li sub-lattice in these high Li content tetragonal systems, thus highlighting the need for Li contents lower than 7 to achieve high Li ion conductivities in these garnet systems.

4. Conclusions

In this paper, we have shown the successful synthesis of the high Li content garnet phases $LnSr_2Ta_2Li_7O_{12}$ (Ln = La, Pr, Nd, Sm, Gd). The X-ray diffraction data confirm the adoption of the tetragonal garnet structure in these systems, thus providing confirmation that "Li_7" garnet systems prefer to adopt this ordered structure, which can be attributed to the fact that it limits too short Li-Li interactions. From VT-XRD and TGA studies, there was evidence for partial H^+/Li^+ exchange occurring in these samples on being left in air, even within closed containers, thus showing the need to consider the effect of moisture when characterising garnet Li ion conductors. The conductivity results provide further support to conclusions that the upper limit of 7 Li per formula unit in garnet systems is detrimental to the Li ion conductivity, due to the required ordering on the Li sublattice to accommodate this high Li content.

Acknowledgements

We would like to thank EPSRC and the University of Birmingham for the financial support (M. Howard studentship).

The Bruker D8 diffractometer used in the RT PXRD studies and the Netzsch STA 449 F1 Jupiter Thermal Analyser, used in this research were obtained through Science City Advanced Materials project; Creating and Characterising Next generation Advanced Materials project, with support from Advantage West Midlands (AWM) and part funded by the European regional Development Fund.

Table 1. Calculated tetragonal cell parameters for $LnSr_2Ta_2Li_7O_{12}$ (Ln = La, Pr, Nd, Sm, Gd)

Material	**a (Å)**	**c (Å)**	**Unit Cell Volume (Å^3)**
$LaSr_2Ta_2Li_7O_{12}$	13.0988(7)	12.480(1)	2141.4(2)
$PrSr_2Ta_2Li_7O_{12}$	13.0289(6)	12.439(1)	2111.6(2)
$NdSr_2Ta_2Li_7O_{12}$	13.0244(3)	12.4228(4)	2107.3(1)
$SmSr_2Ta_2Li_7O_{12}$	12.9965(6)	12.425(1)	2098.7(2)
$GdSr_2Ta_2Li_7O_{12}$	12.9206(1)	12.454(1)	2079.1(1)

Figure Caption List

Fig. 1. X-ray diffraction patterns of a) $NdSr_2Ta_2Li_7O_{12}$ b) $SmSr_2Ta_2Li_7O_{12}$ c) $GdSr_2Ta_2Li_7O_{12}$ (arrow indicating impurity Perovskite type phase), and (d) tetragonal $La_3Zr_2Li_7O_{12}$ for comparison

Fig. 2. Variable temperature PXRD patterns from room temperature to 900 °C for $NdSr_2Ta_2Li_7O_{12}$ a) 1st heating b) 1st cooling c) 2nd heating d) 2nd cooling

Fig. 3. a) Temperature dependence of the calculated wt%. of cubic phase for $NdSr_2Ta_2Li_7O_{12}$ b) temperature dependence of tetragonality (c/a ratio) for the tetragonal $NdSr_2Ta_2Li_7O_{12}$ phase

Fig. 4. a) Temperature dependence of the calculated wt%. of cubic phase for $PrSr_2Ta_2Li_7O_{12}$ b) temperature dependence of tetragonality (c/a ratio) for the tetragonal $PrSr_2Ta_2Li_7O_{12}$ phase

Fig. 5. SEM images of a pellet made $NdSr_2Ta_2Li_7O_{12}$ sintered at 1000 °C for 2h. (a)-(c) top view of the pellet, (d)-(f) cross section of the pellet broken in the middle.

Fig. 6. Arrhenius plots of $LnSr_2Ta_2Li_7O_{12}$ (Ln = La, Pr, Nd, Sm, Gd) in the temperature range 150 - 300°C

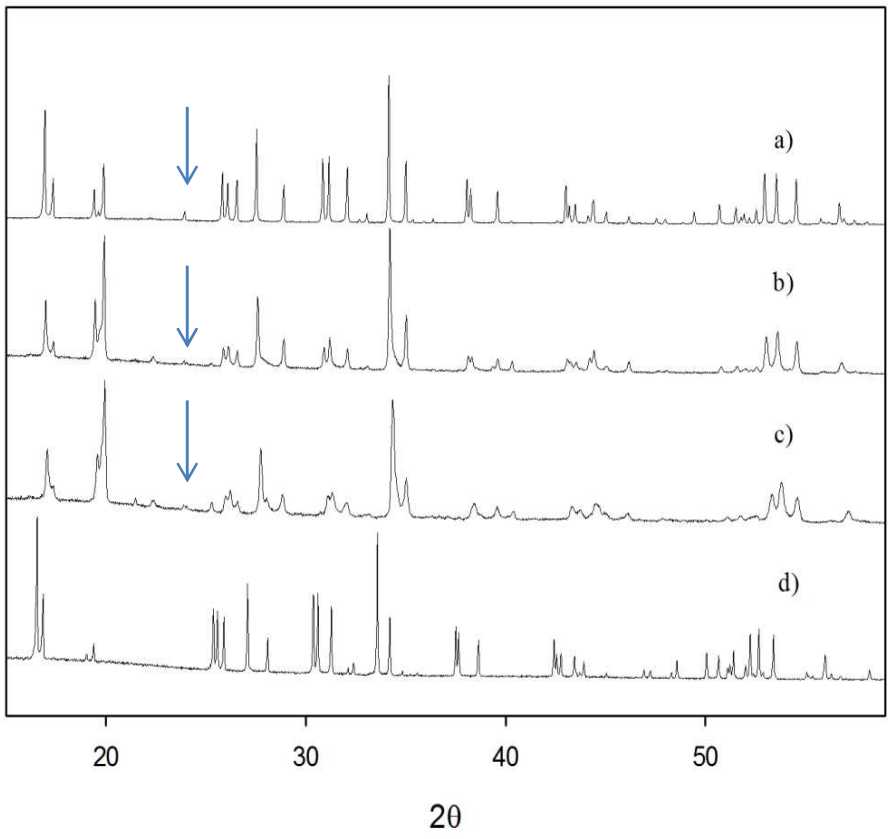

Fig. 1. X-ray diffraction patterns of a) $NdSr_2Ta_2Li_7O_{12}$ b) $SmSr_2Ta_2Li_7O_{12}$ c) $GdSr_2Ta_2Li_7O_{12}$ (arrow indicating impurity Perovskite type phase), and (d) tetragonal $La_3Zr_2Li_7O_{12}$ for comparison

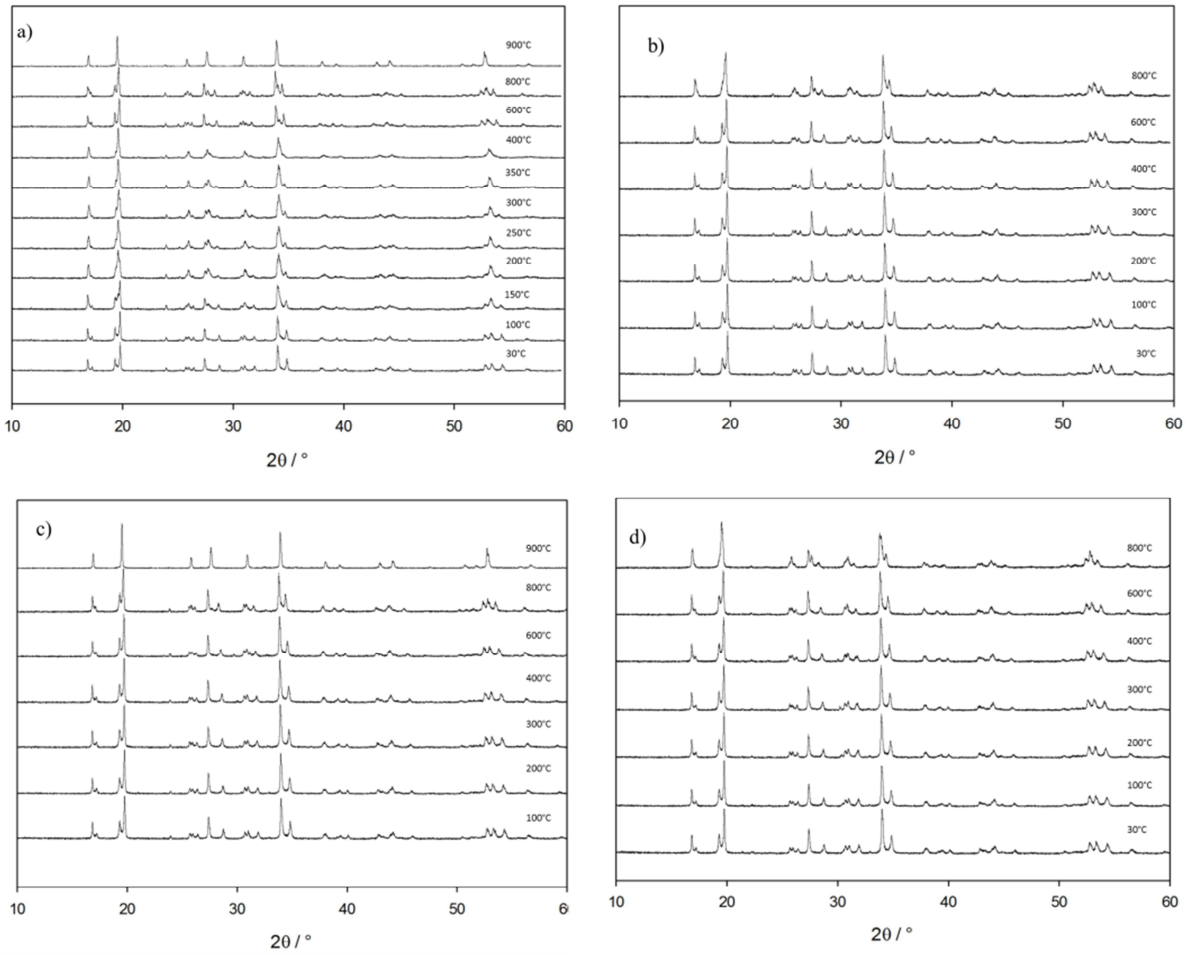

Fig. 2**.** Variable temperature PXRD patterns from room temperature to 900 °C for $NdSr_2Ta_2Li_7O_{12}$ a) 1st heating b) 1st cooling c) 2nd heating d) 2nd cooling

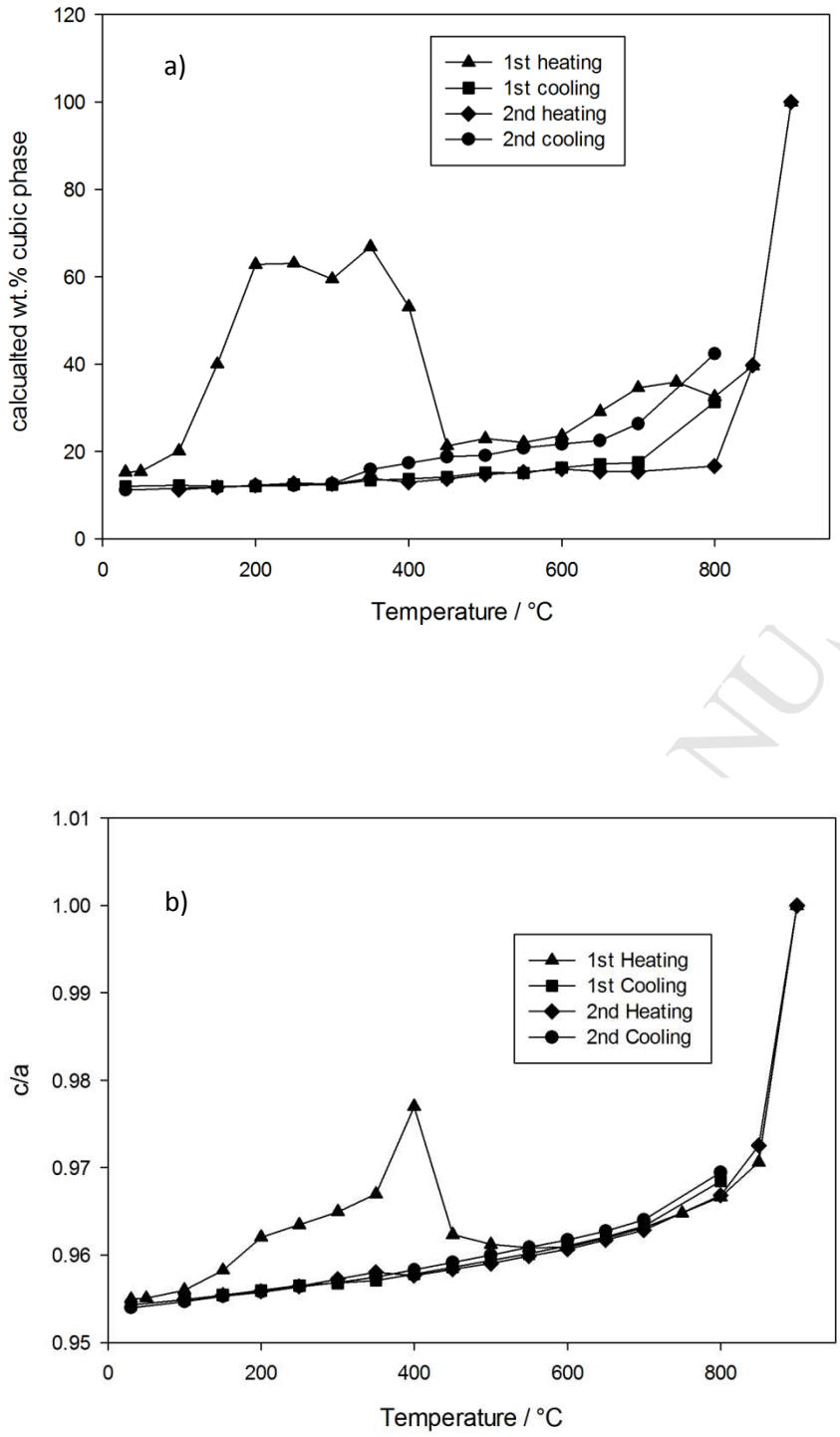

Fig. 3. a) Temperature dependence of the calculated wt%. of cubic phase for $NdSr_2Ta_2Li_7O_{12}$ b) temperature dependence of tetragonality (c/a ratio) for the tetragonal $NdSr_2Ta_2Li_7O_{12}$ phase

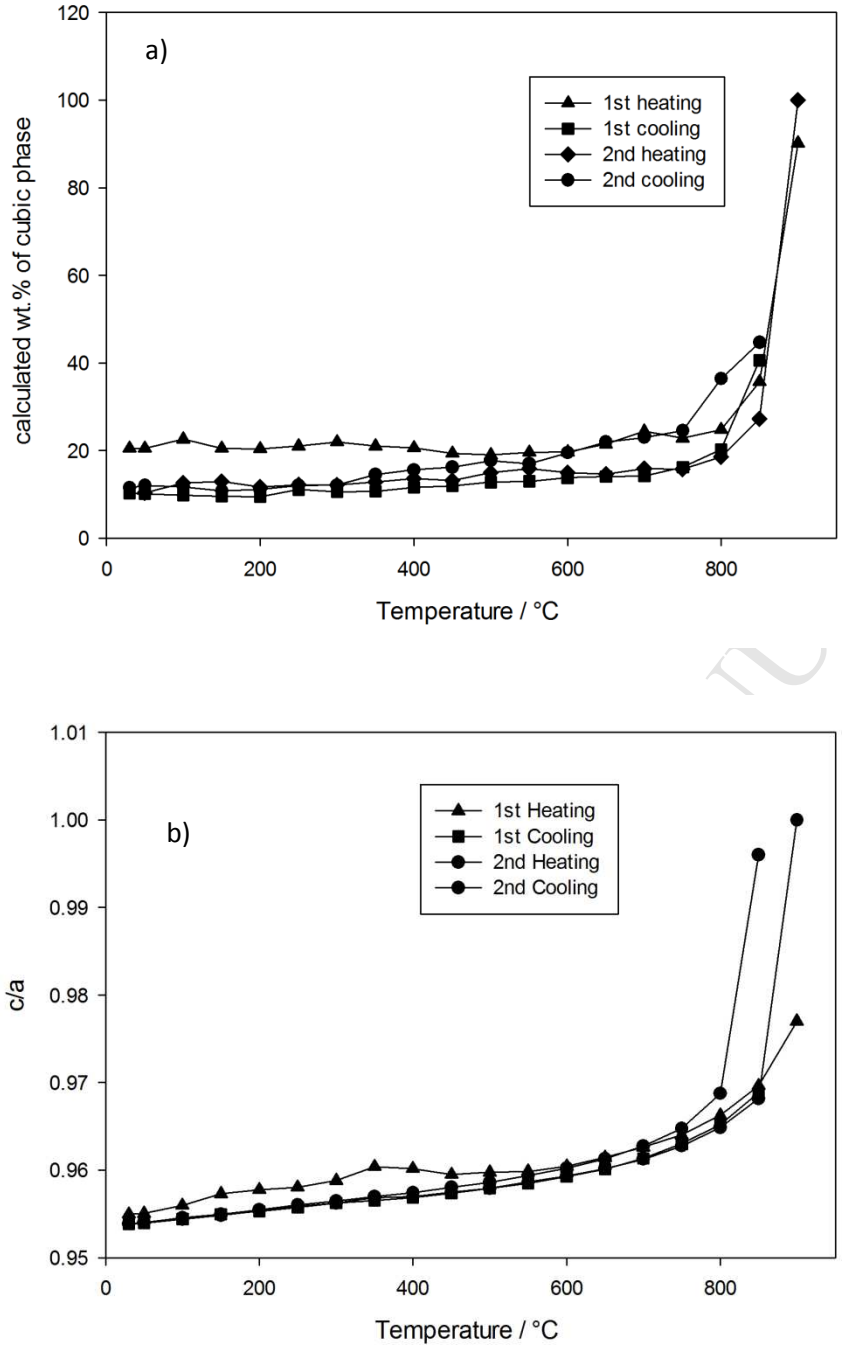

Fig. 4. a) Temperature dependence of the calculated wt%. of cubic phase for $PrSr_2Ta_2Li_7O_{12}$ b) temperature dependence of tetragonality (c/a ratio) for the tetragonal $PrSr_2Ta_2Li_7O_{12}$ phase

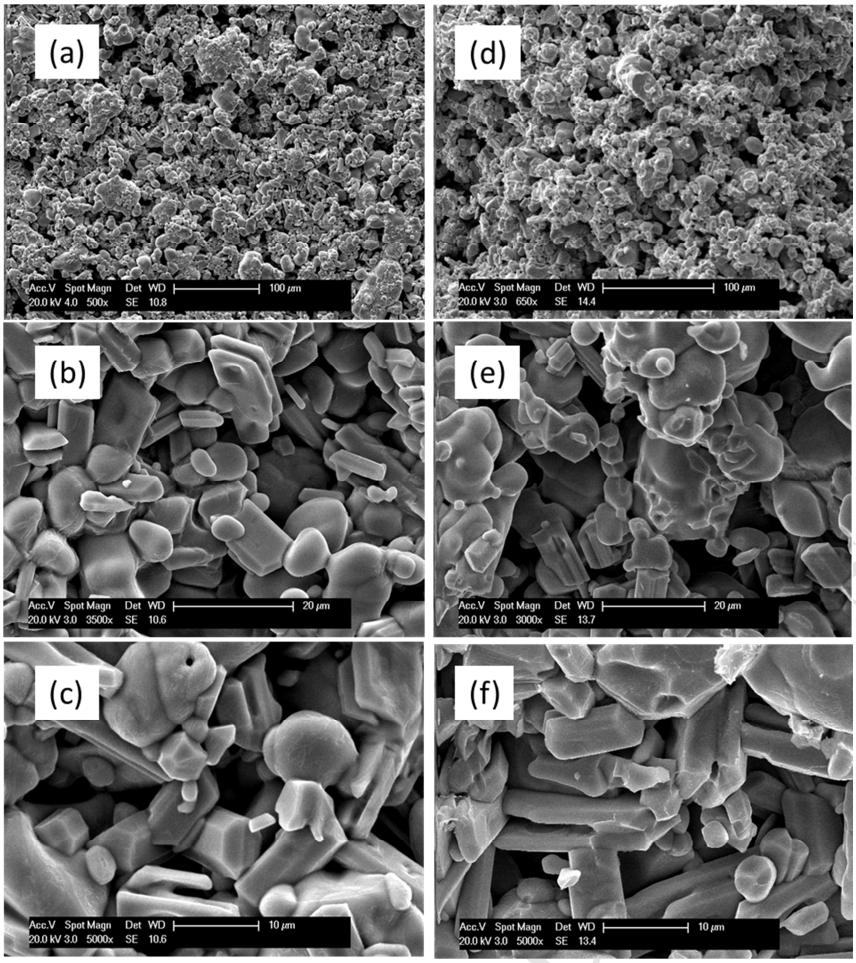

Fig. 5. SEM images of a pellet made $NdSr_2Ta_2Li_7O_{12}$ sintered at 1000 °C for 2h. (a)-(c) top view of the pellet, (d)-(f) cross section of the pellet broken in the middle.

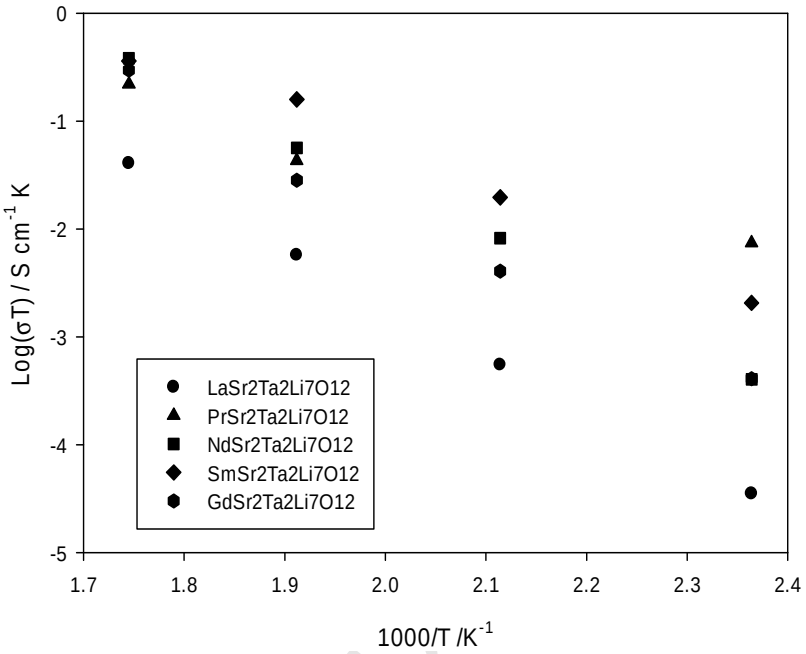

Fig. 6. Arrhenius plots of $LnSr_2Ta_2Li_7O_{12}$ (Ln = La, Pr, Nd, Sm, Gd) in the temperature range 150-300°C

References

[1] V. Thangadurai, S. Adams, W. Weppner, Crystal structure revision and identification of Li^+-ion migration pathways in the garnet-like $Li_5La_3M_2O_{12}$ (M = Nb, Ta) oxides, Chem. Mater. 16 (2004) 2998-3006.

[2] E.J. Cussen, The structure of lithium garnets: cation disorder and clustering in a new family of fast Li^+ conductors, Chem. Commun. 4 (2006) 412-413.

[3] M.P. O'Callaghan, E.J. Cussen, Lithium dimer formation in the Li-conducting garnets $Li_{5+x}Ba_xLa_{3-x}Ta_2O_{12}$ ($0 < x \leq 1.6$), Chem. Commun. 20 (2007) 2048-2050.

[4] J. Percival, P.R. Slater, Identification of the Li sites in the Li ion conductor, $Li_6SrLa_2Nb_2O_{12}$, through neutron powder diffraction studies, Solid State Commun. 142 (2007) 355-357.

[5] J. Percival, E. Kendrick, P.R. Slater, Synthesis and conductivities of the gamet-related Li ion conductors, $Li_5Ln_3Sb_2O_{12}$ (Ln=La, Pr, Nd, Sm, Eu), Solid State Ionics 179 (2008) 1666-1669.

[6] J. Percival, D. Apperley, P.R. Slater, Synthesis and structural characterisation of the Li ion conducting garnet-related systems, $Li_6ALa_2Nb_2O_{12}$ (A = Ca, Sr), Solid State Ionics 179 (2008) 1693-1696.

[7] J. Percival, E. Kendrick, R.I. Smith, P.R. Slater, Cation ordering in Li containing garnets: synthesis and structural characterisation of the tetragonal system, $Li_7La_3Sn_2O_{12}$, Dalton. Trans. 26 (2009) 5177-5181.

[8] J. Awaka, N. Kijima, Y. Takahashi, H. Hayakawa, J. Akimoto, Synthesis and crystallographic studies of garnet-related lithium-ion conductors $Li_6CaLa_2Ta_2O_{12}$ and $Li_6BaLa_2Ta_2O_{12}$, Solid State Ionics 180 (2009) 602-606.

[9] J. Awaka, N. Kijima, H. Hayakawa, J. Akimoto, Synthesis and structure analysis of tetragonal $Li_7La_3Zr_2O_{12}$ with the garnet-related type structure, J. Solid State Chem. 182 (2009) 2046-2052.

[10] S. Narayanan, V. Thangadurai, Effect of Y substitution for Nb in $Li_5La_3Nb_2O_{12}$ on Li ion conductivity of garnet-type solid electrolytes, J. Power Sources 196 (2011) 8085-8090.

[11] A. Kuhn, S. Narayanan, L. Spencer, G. Goward, V. Thangadurai, M. Wilkening, Li self-diffusion in garnet-type $Li_7La_3Zr_2O_{12}$ as probed directly by diffusion-induced ^7Li spin-lattice relaxation NMR spectroscopy, Phys. Rev. B 83 (2011) 094302 1-11.

[12] V. Thangadurai, H. Kaack, W.J.F. Weppner, Novel fast lithium ion conduction in garnet-type $Li_5La_3M_2O_{12}$ (M = Nb, Ta), J. Am. Ceram. Soc. 86 (2003) 437-440.

[13] V. Thangadurai, W. Weppner, Effect of sintering on the ionic conductivity of garnet-related structure $Li_5La_3Nb_2O_{12}$ and In- and K-doped $Li_5La_3Nb_2O_{12}$, J. Solid State Chem. 179 (2006) 974-984.

[14] D. Mazza, Remarks on a ternary phase in the La_2O_3-Nb_2O_5-Li_2O, La_2O_3-Ta_2O_5-Li_2O system, Mater. Lett. 7 (1988) 205-207.

[15] E.J. Cussen, T.W.S. Yip, G. O'Neill, M.P. O'Callaghan, A comparison of the transport properties of lithium-stuffed garnets and the conventional phases $Li_3Ln_3Te_2O_{12}$, J. Solid State Chem. 184 (2011) 470-475.

[16] V. Thangadurai, D. Pinzaru, S. Narayanan, A.K. Baral, Fast Solid-State Li Ion Conducting Garnet-Type Structure Metal Oxides for Energy Storage, J. Phys. Chem. Lett. 6 (2015) 292-299.

[17] M.A. Howard, O. Clemens, E. Kendrick, K.S. Knight, D.C. Apperley, P.A. Anderson, P.R. Slater, Effect of Ga incorporation on the structure and Li ion conductivity of $La_3Zr_2Li_7O_{12}$, Dalton. Trans. 41 (2012) 12048-12053.

[18] M.A. Howard, O. Clemens, K.S. Knight, P.A. Anderson, S. Hafiz, P.M. Panchmatia, P.R. Slater, Synthesis, conductivity and structural aspects of $Nd_3Zr_2Li_{7-3x}Al_xO_{12}$, J. Mater. Chem. A 1 (2013) 14013-14022.

[19] J. Awaka, N. Kijima, K. Kataoka, H. Hayakawa, K.-i. Ohshima, J. Akimoto, Neutron powder diffraction study of tetragonal $Li_7La_3Hf_2O_{12}$ with the garnet-related type structure, J. Solid State Chem. 183 (2010) 180-185.

[20] R. Murugan, V. Thangadurai, W. Weppner, Fast Lithium Ion Conduction in Garnet-Type $Li_7La_3Zr_2O_{12}$, Angew. Chem. Int. Ed. 46 (2007) 7778-7781.

[21] M. Huang, A. Dumon, C.-W. Nan, Effect of Si, In and Ge doping on high ionic conductivity of $Li_7La_3Zr_2O_{12}$, Electrochem. Commun. 21 (2012) 62-64.

[22] J. Wolfenstine, J. Ratchford, E. Rangasamy, J. Sakamoto, J.L. Allen, Synthesis and high Li-ion conductivity of Ga-stabilized cubic $Li_7La_3Zr_2O_{12}$, Mater. Chem. Phys. 134 (2012) 571-575.
[23] J.L. Allen, J. Wolfenstine, E. Rangasamy, J. Sakamoto, Effect of substitution (Ta, Al, Ga) on the conductivity of $Li_7La_3Zr_2O_{12}$, J. Power Sources 206 (2012) 315-319.
[24] J. Wolfenstine, J. Sakamoto, J.L. Allen, Electron microscopy characterization of hot-pressed Al substituted $Li_7La_3Zr_2O_{12}$, J. Mater. Sci. 47 (2012) 4428-4431.
[25] E. Rangasamy, J. Wolfenstine, J. Sakamoto, The role of Al and Li concentration on the formation of cubic garnet solid electrolyte of nominal composition $Li_7La_3Zr_2O_{12}$, Solid State Ionics 206 (2012) 28-32.
[26] A. Kuhn, J.-Y. Choi, L. Robben, F. Tietz, M. Wilkening, P. Heitjans, Li Ion Dynamics in Al-Doped Garnet-Type $Li_7La_3Zr_2O_{12}$ Crystallizing with Cubic Symmetry, Z. Phys. Chem. 226 (2012) 525-537.
[27] M. Huang, W. Xu, Y. Shen, Y.H. Lin, C.W. Nan, X-ray absorption near-edge spectroscopy study on Ge-doped $Li_7La_3Zr_2O_{12}$: enhanced ionic conductivity and defect chemistry, Electrochim. Acta. 115 (2014) 581-586.
[28] C. Bernuy-Lopez, W. Manalastas, J.M.L. del Amo, A. Aguadero, F. Aguesse, J.A. Kilner, Atmosphere Controlled Processing of Ga-Substituted Garnets for High Li-Ion Conductivity Ceramics, Chem. Mater. 26 (2014) 3610-3617.
[29] D. Rettenwander, C.A. Geiger, M. Tribus, P. Tropper, G. Amthauer, A Synthesis and Crystal Chemical Study of the Fast Ion Conductor $Li_{7-3x}Ga_xLa_3Zr_2O_{12}$ with x=0.08 to 0.84, Inorg. Chem. 53 (2014) 6264-6269.
[30] S. Mukhopadhyay, T. Thompson, J. Sakamoto, A. Huq, J. Wolfenstine, J.L. Allen, N. Bernstein, D.A. Stewart, M.D. Johannes, Structure and Stoichiometry in Supervalent Doped $Li_7La_3Zr_2O_{12}$, Chem. Mater. 27 (2015) 3658-3665.
[31] E. Hanc, W. Zajac, J. Molenda, Synthesis procedure and effect of Nd, Ca and Nb doping on structure and electrical conductivity of $Li_7La_3Zr_2O_{12}$ garnets, Solid State Ionics 262 (2014) 617-621.
[32] L. Dhivya, N. Janani, B. Palanivel, R. Murugan, Li^+ transport properties of W substituted $Li_7La_3Zr_2O_{12}$ cubic lithium garnets, AIP. Adv. 3 (2013) 082115 1-21.
[33] Y.X. Wang, W. Lai, High Ionic Conductivity Lithium Garnet Oxides of $Li_{7-x}La_3Zr_{2-x}Ta_xO_{12}$ Compositions, Electrochem. Solid State Lett. 15 (2012) A68-A71.
[34] G.T. Hitz, E.D. Wachsman, V. Thangadurai, Highly Li-Stuffed Garnet-Type $Li_{7+x}La_3Zr_{2-x}Y_xO_{12}$, J. Electrochem. Soc. 160 (2013) A1248-A1255.
[35] K. Ishiguro, Y. Nakata, M. Matsui, I. Uechi, Y. Takeda, O. Yamamoto, N. Imanishi, Stability of Nb-Doped Cubic $Li_7La_3Zr_2O_{12}$ with Lithium Metal, J. Electrochem. Soc. 160 (2013) A1690-A1693.
[36] S. Song, B. Yan, F. Zheng, D. Hai Minh, L. Lu, Crystal structure, migration mechanism and electrochemical performance of Cr-stabilized garnet, Solid State Ionics 268 (2014) 135-139.
[37] T. Thompson, J. Wolfenstine, J.L. Allen, M. Johannes, A. Huq, I.N. David, J. Sakamoto, Tetragonal vs. cubic phase stability in Al - free Ta doped $Li_7La_3Zr_2O_{12}$ (LLZO), J. Mater. Chem. A 2 (2014) 13431-13436.
[38] P. Bottke, D. Rettenwander, W. Schmidt, G. Amthauer, M. Wilkening, Ion Dynamics in Solid Electrolytes: NMR Reveals the Elementary Steps of Li^+ Hopping in the Garnet $Li_{6.5}La_3Zr_{1.75}Mo_{0.25}O_{12}$, Chem. Mater. 27 (2015) 6571-6582.
[39] D. Wang, G. Zhong, W.K. Pang, Z. Guo, Y. Li, M.J. McDonald, R. Fu, J.-X. Mi, Y. Yang, Toward Understanding the Lithium Transport Mechanism in Garnet-type Solid Electrolytes: Li^+ Ion Exchanges and Their Mobility at Octahedral/Tetrahedral Sites, Chem. Mater. 27 (2015) 6650-6659.
[40] T. Thompson, A. Sharafi, M.D. Johannes, A. Huq, J.L. Allen, J. Wolfenstine, J. Sakamoto, A Tale of Two Sites: On Defining the Carrier Concentration in Garnet-Based Ionic Conductors for Advanced Li Batteries, Adv. Energy Mater. 5 (2015) 1500096 1-9.
[41] K. Yoshima, Y. Harada, N. Takami, Thin hybrid electrolyte based on garnet-type lithium-ion conductor $Li_7La_3Zr_2O_{12}$ for 12 V-class bipolar batteries, J. Power Sources 302 (2016) 283-290.
[42] F. Du, N. Zhao, Y. Li, C. Chen, Z. Liu, X. Guo, All solid state lithium batteries based on lamellar garnet-type ceramic electrolytes, J. Power Sources 300 (2015) 24-28.
[43] L.Truong, V. Thangadurai, First Total H^+/Li^+ Ion Exchange in Garnet-Type $Li_5La_3Nb_2O_{12}$ Using Organic Acids and Studies on the Effect of Li Stuffing, Inorg. Chem. 51 (2012) 1222-1224.

[44] L. Truong, M. Howard, O. Clemens, K.S. Knight, P.R. Slater, V. Thangadurai, Facile proton conduction in H^+/Li^+ ion-exchanged garnet-type fast Li-ion conducting $Li_5La_3Nb_2O_{12}$, J. Mater. Chem. A 1 (2013) 13469-13475.
[45] L. Truong, V. Thangadurai, Soft-Chemistry of Garnet-Type $Li_{5+x}Ba_xLa_{3-x}Nb_2O_{12}$ (x=0, 0.5, 1): Reversible $H^+ \leftrightarrow Li^+$ Ion-Exchange Reaction and Their X-ray, ^7Li MAS NMR, IR, and AC Impedance Spectroscopy Characterization, Chem. Mater. 23 (2011) 3970-3977.
[46] H. Nemori, Y. Matsuda, S. Mitsuoka, M. Matsui, O. Yamamoto, Y. Takeda, N. Imanishi, Stability of garnet-type solid electrolyte $Li_xLa_3A_{2-y}B_yO_{12}$ (A = Nb or Ta, B = Sc or Zr), Solid State Ionics 282 (2015) 7-12.
[47] C. Galven, J.L. Fourquet, M.P. Crosnier-Lopez, F. Le Berre, Instability of the Lithium Garnet $Li_7La_3Sn_2O_{12}$: Li^+/H^+ Exchange and Structural Study, Chem. Mater 23 (2011) 1892-1900.
[48] G. Larraz, A. Orera, M.L. Sanjuan, Cubic phases of garnet-type $Li_7La_3Zr_2O_{12}$: the role of hydration, J. Mater. Chem. A 1 (2013) 11419-11428.
[49] C. Galven, J. Dittmer, E. Suard, F. Le Berre, M.P. Crosnier-Lopez, Instability of Lithium Garnets against Moisture. Structural Characterization and Dynamics of $Li_{7-x}H_xLa_3Sn_2O_{12}$ and $Li_{5-x}H_xLa_3Nb_2O_{12}$, Chem. Mater. 24 (2012) 3335-3345.
[50] G. Larraz, A. Orera, J. Sanz, I. Sobrados, V. Diez-Gomez, M.L. Sanjuan, NMR study of Li distribution in $L_{i7-x}H_xLa_3Zr_2O_{12}$ garnets, J. Mater. Chem. A 3 (2015) 5683-5691.
[51] A. Coelho, Topas Academic v4.1 Computer Software, Brisbane, 2007.
[52] R. Murugan, V. Thangadurai, W. Weppner, Lattice parameter and sintering temperature dependence of bulk and grain-boundary conduction of garnet-like solid Li-electrolytes, J. Electrochem. Soc. 155 (2008) A90-A101.
[53] R.W. Cheary, A.A. Coelho, J.P. Cline, Fundamental parameters line profile fitting in laboratory diffractometers, J. Res. Natl. Inst. Stan. 109 (2004) 1-25.
[54] D. Johnson, ZView: a Software Program for IES Analysis 2.8, Scribner Associates Inc., Southern Pines, NC, 2008.
[55] J. Percival, E. Kendrick, P.R. Slater, Synthesis and characterisation of the garnet-related Li ion conductorl $Li_5Nd_3Sb_2O_{12}$, Mater. Res. Bull. 43 (2008) 765-770.

The successful synthesis of new $LnSr_2Ta_2Li_7O_{12}$ (Ln = La, Pr, Nd, Sm, Gd) garnet phases

The demonstration that these “Li7” garnets all adopt tetragonal symmetry consistent with Li ordering

The demonstration that these systems are susceptible to moisture from the air, which leads to partial H/Li Exchange